Available online at www.sciencedirect.com
ScienceDirect
Microporous and Mesoporous Materials 111 (2008) 300–306
MICROPOROUS AND MESOPOROUS MATERIALS
www.elsevier.com/locate/micromeso

Incorporation of Ag nanostructures into channels of nitrided mesoporous silica

Yinfeng Zhao [a,b], Yue Qi [a], Yingxu Wei [a], Yangyang Zhang [a,b], Shigang Zhang [a,b], Yue Yang [a], Zhongmin Liu [a,*]

[a] *Applied Catalysis Laboratory, Dalian Institute of Chemical Physics, Chinese Academy of Sciences, P.O. Box 110, Dalian 116023, PR China*
[b] *Graduate School of the Chinese Academy of Sciences, Beijing 100039, PR China*

Received 8 March 2007; received in revised form 3 July 2007; accepted 8 August 2007
Available online 15 August 2007

Abstract

Nitrided mesoporous silica was used as a host for accommodating nano-silver into the channels. The nitridation of the mesoporous silica host, i.e. SBA-15, with ammonia caused the generation of $-NH_x$ groups on the surface. The following impregnation of the nitrided SBA-15 with aqueous $AgNO_3$ solution and further reduction led to formation of silver nanostructures in the channels. The samples were characterized by FTIR, XRD, TEM and XPS techniques. The impregnation time has effect on the morphology of the resulting nanostructures. The interaction between silver species and surface $-NH_x$ was the key to immobilize Ag in the channels. A scheme was proposed to illustrate the synthesis of Ag nanostructures using nitrided mesoporous host.

Keywords: Silver nanostructures; Nitridation; SBA-15; Host

1. Introduction

Solid materials embodied with metallic nanostructures have attracted much attention in recent years due to their potential applications in catalysis, semiconductors, ferrofluids, adsorbents, miniaturized electronic and optical devices [1,2]. Porous materials, such as carbon nanotubes [3,4], anodic alumina membranes [5–7], and mesoporous materials [8] have been used as hosts for fabricating this class of materials. Among these hosts, mesoporous silica such as MCM-41 [9] and SBA-15 [10] are often used owing to their specific properties, i.e., large surface area, variable pore diameter and long-range order, etc. The nanostructures of metals (wires or particles) can be confined in the channels of mesoporous silica, thus kept in nano-scale.

Up to now, the nano-metal/silica composites had been prepared via several methods, such as chemical vapour deposition of metal compounds [11,12], ion exchange with metal ions [13,14], addition of metal compounds [15] or nanoparticles [16] in sol–gel mixture and impregnation with metal salts [17–21]. One of the most commonly used methods is to introduce metal ions into the channels of the hosts by impregnation and then reduce the metal species to form nanostructures. However, the interaction between silica surface and the metal precursor is usually weak, so the metal species in the channels are prone to migrate and agglomerate on the outer surface during the impregnation and reduction procedures [17].

To conquer the difficulty of immobilizing metal ions in the channels of mesoporous silica, several strategies have been adopted. Huang et al. reported the preparation of Ag nanowires within mesoporous silica by adding less polar ethanol into the aqueous solvent of silver salts [20]. The selection of $EtOH/H_2O$ proportion was found critical to the formation of Ag nanowires. Han synthesized uniform Ag nanowires within the nano-scale channels of SBA-15 by post-treating the salt-impregnated hosts with CH_2Cl_2 to immobilize metals [21]. Comparatively, a more

* Corresponding author. Tel.: +86 411 8468 5510; fax: +86 411 8469 1570.
E-mail address: liuzm@dicp.ac.cn (Z. Liu).

1387-1811/$ - see front matter © 2007 Elsevier Inc. All rights reserved.
doi:10.1016/j.micromeso.2007.08.004

commonly adopted strategy is to modify the host surface before impregnation with organic compounds which contain certain functional groups such as amines or thiols [22–26]. Shi et al. [27] used 3-aminopropyltrimethoxysilane to modify the surface of mesoporous silica, and then incorporated silver nanoparticles into the channels. The metals can be immobilized by the co-ordination between metal species and amine ligands anchored on the host surface [28,29]. However, these organic compounds are usually toxic, expensive and environmental-unfriendly. Besides, to achieve better incorporation, anhydrous condition is strictly requested in modification and following incorporation procedures.

Here, we present for the first time using nitrided SBA-15 as s host to embody Ag nanostructures. The nitrided silica materials have attracted much attention recently as a new class of solid bases. Previous study showed that during the nitridation the N atoms would substitute for O atoms in frameworks, and give rise to basic sites –NH_xs [30,31]. The new generated surface –NH_x groups are expected to play the same role as the amine groups did in immobilizing metals and in this way the usage of toxic organic amines and solvent could be avoided.

2. Experimental

2.1. Synthesis of the parent SBA-15

The SBA-15 host was synthesized by the method reported elsewhere [10]. Tri-block poly (ethylene oxide) – poly (propylene oxide) – poly (ethylene oxide), $(EO)_{20}(PO)_{70}(EO)_{20}$, was used as template in acidic conditions. For example, 32.0 g of $[(EO)_{20}(PO)_{70}(EO)_{20}]$ was dissolved into the solution of deionized water and 960 g of HCl (2 mol/l), followed by the addition of 68.0 g of tetraethyl orthosilicate slowly. The mixture was maintained at 35–40 °C for 24 h under stirring, and then it was loaded into an autoclave and heated at 100 °C under autogenous pressure for 24 h. The solid product was collected by filtration and washed with deionized water. After dried at 60 °C for 24 h, the solid powder product was calcined in air at 540 °C for 4 h to remove the template.

2.2. Nitridation of the parent SBA-15

Nitridation was carried out by the method reported in the literature [30]. Calcined SBA-15 powder was placed in a tubular quartz furnace. The quartz tube was evacuated and flushed with pure nitrogen to remove the air. Afterwards, the sample was heated at a rate of 5 °C/min in the flow of pure nitrogen. When the temperature reached 400 °C, pure ammonia was introduced with a flow rate of 100 ml/min. Then the furnace temperature was increased to 1000 °C at the maintained heating rate and then held for 20 h. When the nitridation process finished, the sample was cooled to room temperature in a mixture flow of pure nitrogen and ammonia. Then the quartz tube was flushed by pure nitrogen for several hours. The obtained white sample was denoted as SBA-15N. In the sample notation, the suffix 'N' denotes ammonia treatment.

2.3. Formation of silver nanostructures

To synthesize Ag nanostructures inside the mesoporous channels, SBA-15N was first impregnated with 0.1 M $AgNO_3$ aqueous solution under stirring for expected time. Then the solid samples were filtrated and washed with deionized water to remove the excess silver nitrate. The obtained materials were dipped in $NaBH_4$ solution under stirring for several hours to reduce the silver ions. Finally, the samples were filtrated, washed and dried at 110 °C for 12 h. The final products of Ag loaded SBA-15N obtained with different impregnation time of 36 h, 60 h and 72 h were denoted as Ag/SBA-15N-36, Ag/SBA-15N-60 and Ag/SBA-15N-72, respectively. For comparison, non-nitrided SBA-15 was also used as host in the similar Ag incorporating procedure and the product was denoted as Ag/SBA-15.

2.4. Characterization

The nitrogen content of the samples was determined by alkaline digestion with molten NaOH at 400 °C and the resulting NH_3 was titrated with 0.05 M H_2SO_4 aqueous solutions. The detailed procedure was as described in literature [32].

Nitrogen adsorption–desorption isotherms were measured at 77 K on a Micromeritics 2010 apparatus. Before the measurements, the samples were first degassed at 383 K for 3 h and then at 623 K for 5 h under vacuum. The specific surface areas of the samples were calculated with the BET equation. The pore volumes were determined at a P/P_0 value of 0.995. The mean pore diameters were calculated with the BJH equation for the adsorption isotherms.

The infrared (FTIR) spectra were recorded on a Bruker EQUINOX 55 spectrometer by KBr pellet method in the range of 400–4000 cm^{-1} at 4 cm^{-1} resolution and 32 scans.

X-ray diffraction (XRD) patterns were collected on a D/Max-βb X-ray diffractometer equipped with Cu Kα radiation and graphite monochromator. The 2θ angles of small-angle patterns were from 0.5° to 5° at a scan rate of 3°/min. Wide-angle patterns were from 10° to 70° of 2θ at a rate of 20°/min.

Transmission electron microscopy (TEM) and EDX analyses were perfoemed using a JEOL-2000EX electron microscope operating at the accelerating voltage of 120 kV. The samples were pulverized in an agate mortar, ultrasonic dispersed in ethanol and then dropped onto the carbon-coated copper grids prior to the measurement.

X-ray photoelectron spectroscopy (XPS) experiments were performed using a VG ESCALAB MK2 spectrometer equipped with a monochromatic Al Kα X-ray source ($h\nu = 1486.6$ eV). The typical full width at half maximum

(FWHM) of the Ag $3d_{5/2}$ core level photoemission peak is typically 1.15 eV (for metal).

3. Results and discussion

3.1. Surface properties of nitrided SBA-15

The small-angle XRD patterns of the parent and the nitrided SBA-15 are shown in Fig. 1. The parent SBA-15 (Fig. 1a) presents three legible diffraction peaks at 0.84°, 1.48° and 1.7°, respectively, indexed as (100), (110) and (200) reflections of a hexagonal symmetry. For SBA-15N, the three characteristic peaks appear but with lower intensities. Obviously, the ordered mesostructure of SBA-15 is still preserved only with partial deconstruction after high-temperature nitridation at 1000 °C. Though the mesostructure of mesoporous silica material will collapse after heated at 1000 °C in air, it seems that the destruction of the ordered mesostructure would be greatly inhibited in ammonia atmosphere [30,33]. In addition, a decrease on *d* spacing corresponds to the major low angle reflection of nitrided sample, which is usually supposed to be caused by the changes of lattice spacing resulted from the structural rearrangement of SBA-15 at higher temperature [30–34].

The N_2 adsorption–desorption measurement was performed to detect the textural change of the host samples after nitridation. SBA-15N displays a typical type IV isotherm with H2 hysteresis, implying a highly ordered mesostructure (see Supporting information). The textural properties of the samples are summarized in Table 1. Clearly, compared with the original host, the structural parameters of SBA-15N decreased slightly even after high-temperature treatment. The survival of the porosity after nitridation promises the usage of the material as the host for embodying the metal nano-structures.

Fig. 2 gives the IR spectra of the parent and the nitrided hosts. For the parent SBA-15, primary infrared bands related to pure silica SBA-15 framework are ascribed to the asymmetric and symmetric stretching of Si–O–Si at 1086 cm^{-1} and 804 cm^{-1}, respectively [34]. The peaks at 1635 cm^{-1} and 966 cm^{-1} are corresponding to the δ (HOH) of physisorbed water and Si–O stretching vibration of the surface Si–OH groups [30]. On the IR spectrum of SBA-15N, there appeared some typical absorption bands for nitrided silica, stemming from the partial replacement of oxygen atoms by nitrogen atoms to form SiN_xO_y tetrahedrons [30]. The new band at 950 cm^{-1} could be attributed to the stretching of Si–N–Si indicating the incorporation of nitrogen into the framework [30,34]. After thermal treatment under vacuum, the typical OH band due to the absorbance of silanol groups (3740 cm^{-1}) almost disappeared (Fig. 3 Inset), while a broad band assigned to *v* (NH) of ≡SiNHSi≡ [31,35] appeared at about

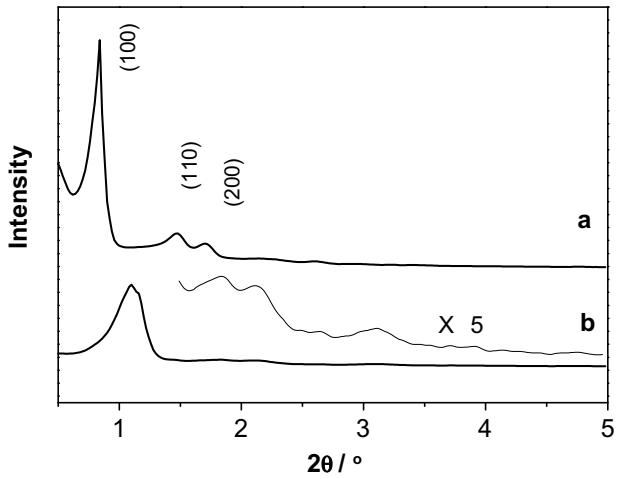

Fig. 1. Small-angle XRD patterns of (a) SBA-15 and (b) SBA-15N.

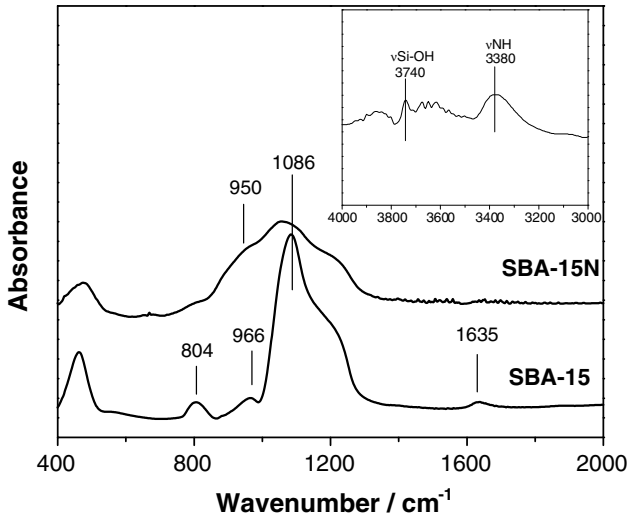

Fig. 2. FTIR spectra (in KBr) of SBA-15 and SBA-5N. Inset: IR spectrum of SBA-15N after thermal treatment under vacuum.

Table 1
The texture properties of silica host and Ag loaded samples

Samples	S_{BET} (m^2/g)	d_p[a] (nm)	V_p[b] (cm^3/g)	N content (wt%)	Ag content (wt%)
SBA-15	598	8.9	0.98	–	–
SBA-15N	499	7.7	0.95	12.2	–
Ag/SBA-15N-36	498	7.7	0.95	8.2	2.4
Ag/SBA-15N-60	459	7.7	0.86	7.4	3.6
Ag/SBA-15N-72	356	7.6	0.81	7.1	4.3

[a] The mean pore sizes of the samples were calculated by the BJH equation using the adsorption isotherms.
[b] The pore volumes of the samples were determined at $P/P_0 = 0.995$.

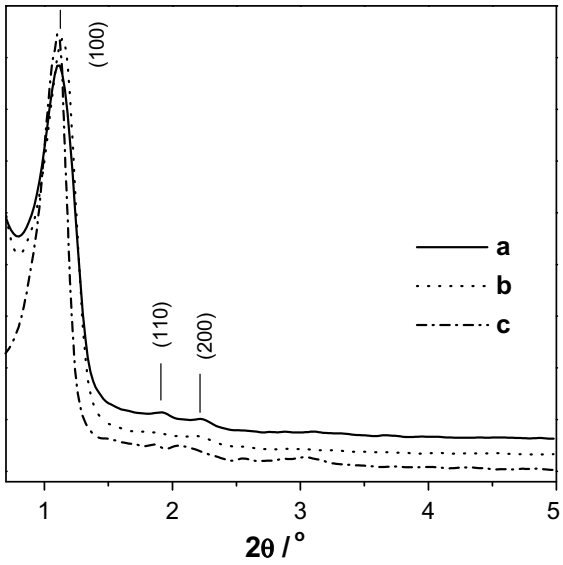

Fig. 3. Small-angle XRD patterns of (a) Ag/SBA-15N-36, (b) Ag/SBA-15N-60 and (c) Ag/SBA-15N-72.

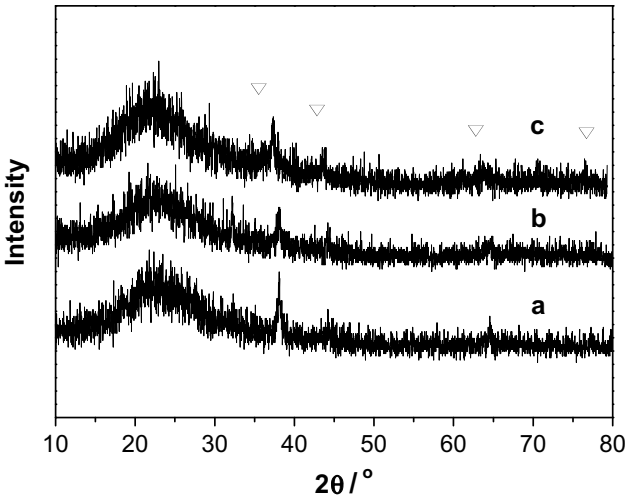

Fig. 4. Wide-angle XRD patterns of (a) Ag/SBA-15N-36, (b) Ag/SBA-15N-60 and (c) Ag/SBA-15N-72.

3390 cm^{-1}. Obviously, after nitridation almost all surface silanol groups might be reacted with ammonia and form $–NH_x$ groups through replacement of surface oxygen atoms by nitrogen atoms. Elemental analysis shows that the SBA-15N sample contains 12.2 wt% of N (Table 1), which confirms almost that 33% oxygen atoms in the parent SBA-15 have been substituted by the nitrogen atoms. Thus, it can be considered that ammonia reacts not only with silanol groups but also with siloxane bonds [30]. So we propose that Si and N are the dominant elements on the surface of the nitrided host.

3.2. Formation of silver nanostructures

After loaded with Ag, the resulted samples presents smaller specific surface areas and pore volumes as listed in Table 1. Besides, as the increase of impregnation time the surface areas and pore volumes of the Ag/SBA-15N samples decreased significantly. However, the mean pore sizes of these samples keep constant after loaded with different amount of Ag. This implies that the Ag species might be incorporated into the mesopores of the host instead of stacked outside. Therefore the Ag loading will decrease the inner surface areas and pore volumes of the resulted samples but have ignoble effect on the mean pore sizes.

The low-angle XRD patterns of silver loaded samples are shown in Fig. 3. Despite impregnant time, all samples display three characteristic (100), (110) and (200) reflections with little change of the peak positions. Thus it can be seen that the silver incorporated procedure has little influence on the ordered mesostructure and the lattice spacing of the nitrided host. However, the peak intensities of the Ag loaded samples decreased compared with the nitrided host, though the reducing electron density contrast would cause an increase in XRD intensity. This suggests the Ag particles have indeed been encapsulated inside the mesopores, and thus the partial filling of the host's mesopores caused the decrease of the reflection intensities [12]. A similar result has also been reported in the Ag/MCM-41 system [37]. On the other hand, the incorporation of silver brought some new diffraction peaks in the high-angle XRD patterns. As shown in Fig. 4, four diffraction peaks appeared at about 38.0°, 44.3°, 64.5° and 77.3°, respectively, corresponding to the (111), (200), (220) and (311) reflections of cubic Ag.

Fig. 5 presents the TEM images of the nitrided host and the silver loaded samples. In accordance with the XRD results (Fig. 1), the mesostructure of the host was preserved after high-temperature nitridation, as the mesoscopic ordering is clearly identified in the TEM view (Fig. 5a). For the Ag/SBA-15N samples, nano-sized Ag particles can be observed (see Fig. 5b–d) and their morphology varied with the impregnation time. Dark dot-like objects appeared in the channels of the host after 36 h impregnation (Fig. 5b). As the impregnation time prolonged, more nod-like objects could be observed at 60 h (Fig. 5c). Long nanowires forms could be found in the channels of the sample, which was impregnated for 72 h. The longitude of these wires are beyond several hundred nanometers (Fig. 5d). The high-magnification image (Fig. 5e) shows that the nanowires are in a uniform diameter, which is close to the pore diameter of SBA-15N.

The elemental analysis of N and Ag contents are also listed in Table 1. The result of EDX analyses showed that the impregnation time has an effect on the silver content. As the time prolonged, the silver content increased. The highest silver content of silver loaded sample was 4.3%, which was obtained after 72 h impregnation. Besides, we found that N content decreased as the increase of impregnation time. When the nitrided host was impregnated with silver precursor for 36 h, the N content of the obtained Ag/SBA-15N-36 was 8.2 wt%. This value decreased about 30%

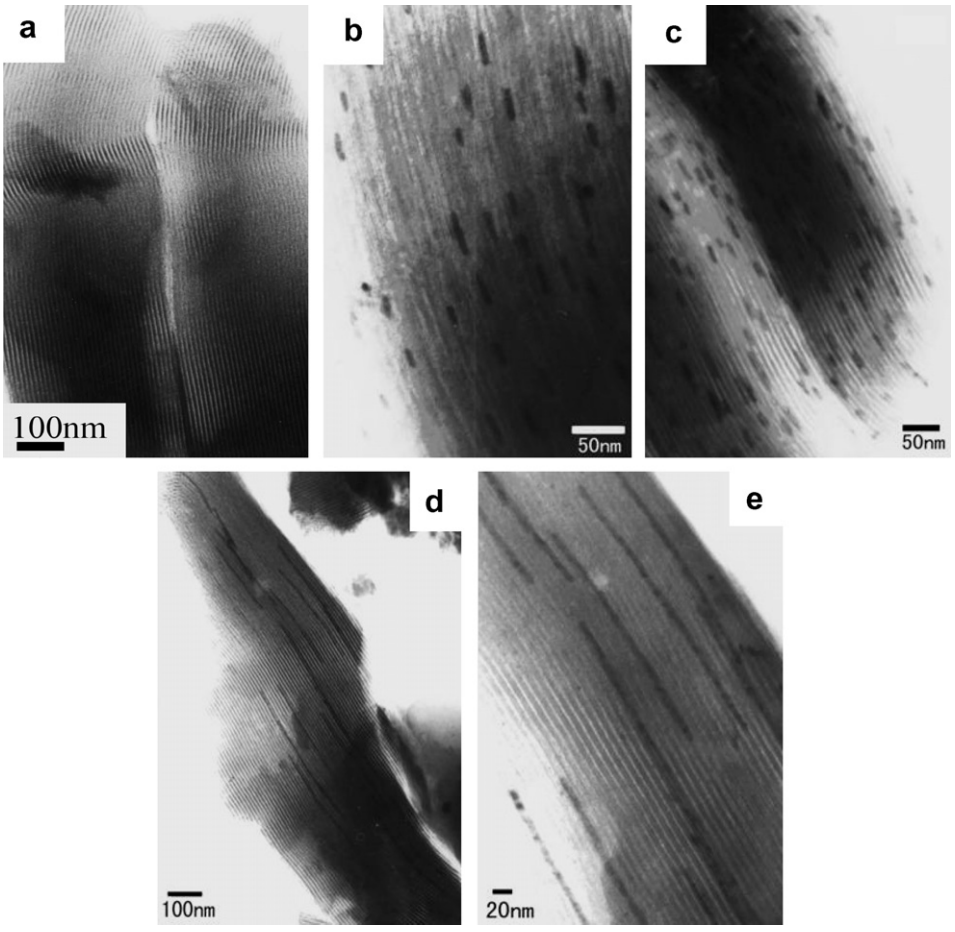

Fig. 5. TEM images of (a) SBA-15N, (b) Ag/SBA-15N-36, (c) Ag/SBA-15N-60, (d) and (e) Ag/SBA-15N-72.

compared with that of the parent SBA-15N (12.2 wt%). The nitrogen losing is more distinct as the increase of the impregnant time. The nitrogen losing should be attributed to the hydrolysis reaction between various ammonium group and water to produce NH_3 and Si–OH [36].

In a comparative test, when non-nitrided SBA-15 was used as the host to load silver by the same procedure as that for SBA-15N, no nanostructure of silver was observed in the TEM view (Fig. 6 for Ag/SBA-15), while many bulky silver particles much larger than the pore size of the host were found on the external surface. These outer silver particles are quite different from the silver loaded SBA-15N in size and morphology (see Fig. 5b–e). Comparing the whole preparation process for Ag/SBA-15 with that for Ag/SBA-15N, the only difference lies in that whether the host was nitrided or not. When silica with no nitridation was used as host, the pre-impregnated Ag species are prone to migrate out of the channels and congregate on the outer surface to form bulky metal after reduction, as has also been reported by other researchers [20,21,27]. The surface modification of the silica host with nitridation should be helpful for the formation of Ag nanostructures in the channels by inhibiting the emigration of impregnated Ag ions out of the SBA-15 channels. Stronger interaction is supposed to exist between the nitrided surface of the host and the silver species.

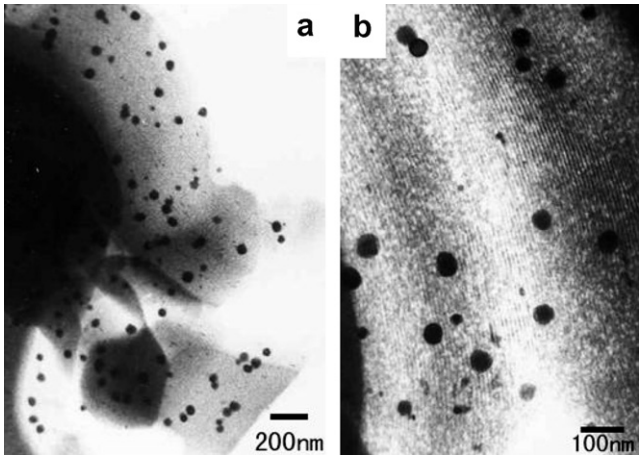

Fig. 6. TEM images of Ag/SBA-15.

The interaction between the nitrided surface and the silver species were studied by X-ray photoelectron spectroscopy (XPS). Table 2 shows the XPS results of sample SBA-15N and Ag/SBA-15N-72. For SBA-15N, the signals

Table 2
XPS data of the silvered SBA-15N and unsilvered SBA-15N

Samples	Elemental environments	Binding energy (eV)
SBA-15N	C 1s	285.0
	N 1s	398.3
	O 1s	532.5
	Si 2p	103.0
Ag/SBA-15N	C 1s	285.0
	N 1s (free)	398.0
	N 1s (coordinated)	399.1
	O 1s	532.3
	Si 2p	103.1
	Ag $3d_{5/2}$	368.2
	Ag $3d_{3/2}$	374.2

corresponding to Si 2p, C 1s, N 1s, and O 1s ionization processes appear at binding energies of ca. 103.0, 285.0, 398.3, and 532.5 eV, respectively. After silver incorporation, the binding energies of Si 2p, C 1s and O 1s did not change, while two new signals appeared at 368.2 eV and 374.2 eV corresponding to Ag $3d_{5/2}$ and Ag $3d_{3/2}$, respectively, which give the information of existence of Ag atoms. Besides these two peaks, a new N 1s signal appeared at 399.1 eV, while the signal at 398.0 eV still remained. Baumgarten and co-workers have reported the appearance of new XPS peak for N 1s of poly-{acrylamide-co-[3-(acryloylamino) propyltrimethylammoniumchloride]} when it was used as host to anchor the platinum ions [29]. This new N 1s peak was believed due to the Pt^{4+} binding to amide and (or) quaternary groups. A stabilization of the platinum through two quaternary and one (or more) amide group was suggested. The platinum complex remained stable even after reduction to Pt^{2+} and Pt^0, as changes in the XPS signal were only minor. Similarly, Chen and co-workers have found a new XPS peak for N 1s [28] when using poly (*N*-isopropylacrylamide)-coated polystyrene microphores as hosts to anchor the Ag ions. The interactions between amine and metal ions caused an increasing binding energy of parts of the N 1s of amine, 0.8–1.0 eV higher than those original. In the present work, the difference between the binding energy of the newly appeared N 1s (399.1 eV) peak and that for original surface NH_x (398.3 eV) is about 1.1 eV. We suppose that this new peak is corresponding to the strong interaction between surface NH_x species and Ag atoms. The nitridation of the host has produced NH_x species on both the inner and the outer surface. In the impregnation procedure, silver ions could be immobilized by the NH_x species on the outer surface as well as the inner surface, even after washed with deionized water. Although the new N 1s signal appeared at 399.1 eV is most likely due to interaction of the outer surface NH_x species and Ag, it is reasonable to suppose that there should be the same interaction between the inner surface NH_x species and the incorporated Ag nanostructures.

As described above, the nitridation of silica host was an important procedure for the incorporation of silver nanostructures. After nitridation, the surface Si–O–Si bonds of the host were at least partially replaced by Si–NH_2 and/or Si–NH–Si bonds. The interaction between the surface NH_x species and the silver species is the key factor for incorporating silver into the channels of the nitrided host. The surface NH_x groups may act as anchors to help immobilizing silver ions in the channels. The interaction between Ag species and the surface NH_x groups, as revealed by the XPS studies, may remain during drying and reduction steps and prevent the diffusion of silver ions from channels to the outer surface. The process of the formation of the nanostructures in the channel of nitrided SBA-15 was proposed in Scheme 1. Different from the commonly used organic grafting method, this nitridation method provide a novel and effective way to incorporate metal nanostructures into the channels of the mesoporous materials.

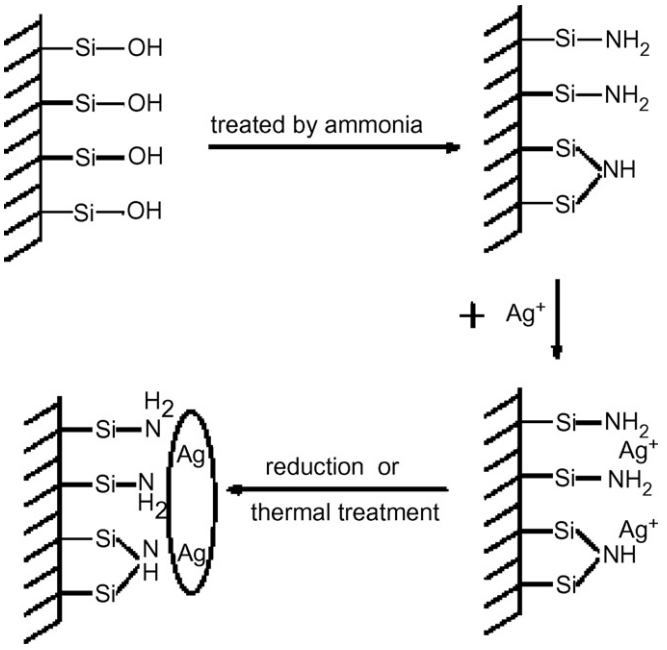

Scheme 1. Schematic illustration of synthesis of Ag nanostructures in the channels of nitrided mesoporous silica.

4. Conclusions

A novel and effective method was developed to fabricate silver nanostructures in the channels of mesoporous materials by using nitrided mesoporous silica as host. After nitridation, the surface of the SBA-15 host was functionalized by the generation of $-NH_x$ groups on the surface. The strong interactions between the $-NH_x$ groups and the sliver atoms would help to anchor the impregnated silver species into the mesoporous channels of the host and corresponding nanostructured-Ag form after reduction. The morphology of silver nanostructures could be controlled in nanoparticle or nanowire by adjusting the impregnation time. This method is expected to be generally applicable to fabricate other metal nanostructures within the channels of mesoporous materials.

Appendix A. Supplementary data

Supplementary data associated with this article can be found, in the online version, at doi:10.1016/j.micromeso.2007.08.004.

References

[1] G. Schmid, M. Bäumle, M. Geerkens, I. Heim, C. Osemann, T. Sawitowski, Chem. Soc. Rev. 28 (1999) 179.
[2] T. Sawitowski, Y. Miquel, A. Heilmann, G. Schmid, Adv. Funct. Mater. 11 (2001) 435.
[3] T. Kyotani, L. Tsai, A. Tomita, Chem. Commun. 7 (1997) 701.
[4] G.G. Wildgoose, C.E. Banks, R.G. Compton, SMALL 2 (2006) 182.
[5] Z.B. Zhang, J.Y. Ying, M.S. Dresselhaus, J. Mater. Res. 13 (1998) 1745.
[6] Z.B. Zhang, D. Gekhtman, M.S. Dresselhaus, J.Y. Ying, Chem. Mater. 11 (1999) 1659.
[7] B.R. Martin, D.J. Dermody, B.D. Reiss, M. Fang, L.A. lyon, M.J. Natan, T.E. Mallouk, Adv. Mater. 11 (1999) 1021.
[8] L.B. Bronstein, Top. Curr. Chem. 226 (2003) 55.
[9] J.S. Beck, C. Vartuli, W.J. Roth, M.E. Leonowicz, C.T. Kresge, K.D. Schmitt, C.T.-W. Chu, D.H. Olson, E.W. Sheppard, S.B. McCullen, J.B. Higgins, J.L. Schlenker, J. Am. Chem. Soc. 114 (1992) 10834.
[10] D. Zhao, Q. Huo, J. Feng, B.F. Chmlka, G.D. Stucky, J. Am. Chem. Soc. 120 (1998) 6024.
[11] C.P. Mehnert, D.W. Weaver, J.Y. Ying, J. Am. Chem. Soc. 120 (1998) 289.
[12] K.B. Lee, S.M. Lee, J. Cheon, Adv. Mater. 13 (2001) 517.
[13] M. Yonemitsu, Y. Tanaka, M. Iwamoto, Chem. Mater. 9 (1997) 2679.
[14] Z. Zhang, S. Dai, X. Fan, D.A. Blom, S.J. Pennycook, Y. Wei, J. Phys. Chem. B 1005 (2001) 6755.
[15] K. Zhu, H. He, S. Xie, X. Zhang, W. Zhou, S. Jin, B. Yue, Chem. Phys. Lett. 377 (2003) 317.
[16] J. Zhu, Z. Kónya, V.F. Puntes, I. Kiricsi, C.X. Miao, J.W. Ager, A.P. Alivisatos, G.A. Somorjai, Langmuir 19 (2003) 4396.
[17] L. Li, J.L. Shi, L.X. Zhang, L.M. Xiong, J.N. Yan, Adv. Mater. 16 (2004) 1079.
[18] H.J. Shin, R. Ryoo, Z. Liu, O. Terasaki, J. Am. Chem. Soc. 123 (2001) 1246.
[19] Z. Zhang, S. Dai, D.A. Blom, J. Shen, Chem. Mater. 14 (2002) 965.
[20] M.H. Huang, A. Choudrey, P. Yang, Chem. Commun. 12 (2000) 1063.
[21] Y.J. Han, J.M. Kim, G.D. Stucky, Chem. Mater. 12 (2000) 2068.
[22] W.H. Zhang, J.L. Shi, L.Z. Wang, D.S. Yan, Chem. Mater. 12 (2000) 1408.
[23] W.H. Zhang, J.L. Shi, H.R. Chen, Z.L. Hua, D.S. Yan, Chem. Mater. 13 (2001) 648.
[24] Y. Guari, C. Thieuleux, A. Mehdi, C. Reye, R.J.P. Corriu, S. Gomez-Gallardo, K. Philippot, B. Chaudret, R. Dutartre, Chem. Commun. 15 (2001) 1374.
[25] H. Wellmann, J. Rathousky, M. Wark, A. Zukal, G. Schulz-Ekloff, Micropor. Mesopor. Mater. 44–45 (2001) 419.
[26] Y. Shan, L. Gao, Mater. Chem. Phys. 89 (2005) 412.
[27] X.G. Zhao, J.L. Shi, B. Hu, L.X. Zhang, Z.L. Hua, Mater. Lett. 58 (2004) 2152.
[28] C. Chen, M. Chen, T. Serizawa, M. Akashi, Adv. Mater. 10 (1998) 1122.
[29] E. Baumgarten, A. Fiebes, A. Stumpe, F. Ronkel, J.W. Schultze, J. Mol. Catal. A 113 (1996) 469.
[30] J. Wang, Q. Liu, Micropor. Mesopor. Mater. 83 (2005) 225.
[31] N. Chino, T. Okubo, Micropor. Mesopor. Mater. 87 (2005) 15.
[32] J.J. Benítez, A. Díaz, Y. Laurent, J.A. Odriozola, Appl. Catal. A 176 (1999) 177.
[33] Y. Xia, R. Mokaya, Angew. Chem. Int. Ed. 42 (2003) 2639.
[34] K. Wan, Q. Liu, C. Zhang, Chem. Lett. 32 (2003) 362.
[35] P. Fink, B. Müller, G. Rudakoff, J. Non-Crystal. Solid 145 (1992) 99.
[36] J. Wang, Q. Liu, J. Mater. Res. 20 (2005) 2296.
[37] P.V. Adhyapak, P. Karandikar, K. Vijayamohanan, A.A. Athawale, A.J. Chandwadkar, Mater. Lett. 58 (2004) 1168.